

Self-Assembly

Self-Assembled Diamide Nanotubes in Organic Solvents**

Nancy Díaz, François-Xavier Simon, Marc Schmutz, Michel Rawiso, Gero Decher, Jacques Jestin, and Philippe J. Mésini*

In the field of nanomaterials, high aspect ratio objects such as fibers and nanotubes are interesting since they can form 3D networklike gels, they can be effectively oriented, and can be used to transport electrons or particles in a 1D fashion. Supramolecular chemistry has proved to be very useful for building such objects. Besides carbon nanotubes and biological macromolecules, many fibrillar structures have been assembled from supramolecular self-association of small molecules.^[1] The self-assembly process offers crucial advantages in the formation of gels by low-mass organic gelators,^[2] such as thermoreversibility, easy processing, and high purity. However, chemical design and synthesis also permits the addition of further functionality to threadlike assemblies for applications such as biomineralization^[3] and the selective binding of protein on lipidic tubes.^[4] Tubular structures offer additional properties because of the presence of an inner cavity, which can be used as nanocargo devices or nano-reactors.^[5] They have also been used to template inorganic tubular structures by sol-gel processes^[6] and multilayered polyelectrolyte tubes upon layer-by-layer adsorption.^[7]

Numerous molecules can self-assemble to form 1D objects such as ribbons or fibrils,^[8] however, only a few of

[*] N. Díaz, F.-X. Simon, Dr. M. Schmutz, Dr. M. Rawiso, Prof. G. Decher, Dr. P. J. Mésini
Institut Charles Sadron
6 rue Boussingault, 67083 Strasbourg Cedex (France)
Fax: (+33) 388-414-099
E-mail: mesini@ics.u-strasbg.fr
Dr. J. Jestin
Laboratoire Léon Brillouin
CEA-Saclay
91191 Gif-sur-Yvette Cedex (France)

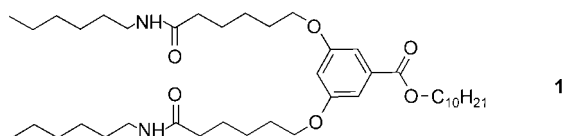
[**] This work was supported by a CONACyT fellowship (N.D.) and by a MESR fellowship (F.-X.S.). We thank Dr. P. Schultz for the use of the cryofracturing apparatus developed by Dr. J.-C. Homo at the IGBMC UMR 7104, Illkirch, France; Benoît Heinrich for WAXS spectra; and Dr. P. Baxter for critical reading of the manuscript.



Supporting information for this article is available on the WWW under <http://www.angewandte.org> or from the author.

them form hollow tubes.^[9] Some such tubes formed from lipids^[10] and bile acids^[11] have diameters on the order of micrometers and are polydisperse. Recent work has enabled the discovery of new self-assembled tubes, such as from sugar derivatives,^[12] bolaamphiphiles,^[13] lipids,^[4] steroids,^[14] peptides,^[15] and hexabenzocoronene derivatives,^[16] with diameters that fill the gap between the micrometer scale and the diameter of the carbon nanotubes (1 to 3 nm). Such tubes are always found along with helical ribbons, which are precursors to the closed tubes and were previously identified by Kunitake and co-workers.^[17] These impressive objects have stimulated much theoretical work in which their assembly into ribbons that can further wind up into helical ribbons, and ultimately form tubes, was modeled.^[18] In relation to the above-mentioned studies, we report a new compound, with a simple chemical structure, which is able to self-assemble into nanotubes in organic solvents. We also report the characterization of these tubes.

Many diamides self-assemble in organic solvents to form fibrillar aggregates through formation of hydrogen-bonding interactions.^[19] The morphology of these aggregates is strongly influenced by the directionality of the hydrogen bonds as well as steric factors. We prepared a diamide bearing a bulky aromatic-decyl ester to study its influence on the shape of the aggregates. Compound **1** was synthesized in two



steps on a gram scale (see Supporting Information) and isolated as a powder that is insoluble at room temperature in most organic solvents (toluene, benzene, alkanes, methanol, ethanol) but soluble in chloroform and dichloromethane. The formation of gels at low concentration was observed when **1** was suspended in aliphatic solvents or toluene, heated until completely dissolved, and the resulting solution cooled back at 25 °C. The formation of the gel could be observed above concentrations of 0.05 wt % in cyclohexane. Gel formation is thermally reversible: heating the gel results in an isotropic sol phase. This behavior arises from the formation of aggregates through reversible bonds.

The nature of these bonds was explored by spectroscopic techniques. Examination of the **1**/cyclohexane gels by FTIR spectroscopy showed an NH stretching band at 3302 cm⁻¹ (Figure 1 a) and an amide I band at 1642 cm⁻¹ (Figure 1 b) characteristic of H-bonded amides. In chloroform, in which **1** is soluble at all concentrations, the IR spectra showed only an H-free NH band at 3450 cm⁻¹ and a CO band at 1663 cm⁻¹. When the gels are heated from 26 to 64 °C, which is above the melting temperature of the gel (59 °C), the amide A band (Figure 1 a) at 3302 cm⁻¹ and the amide I and II bands at 1642 and 1551 cm⁻¹ (Figure 1 b) disappear gradually while shifted bands appear at 3457, 1660, and 1520 cm⁻¹, respectively. These bands are characteristic of H-free amides and their intensities increase with temperature. These measurements

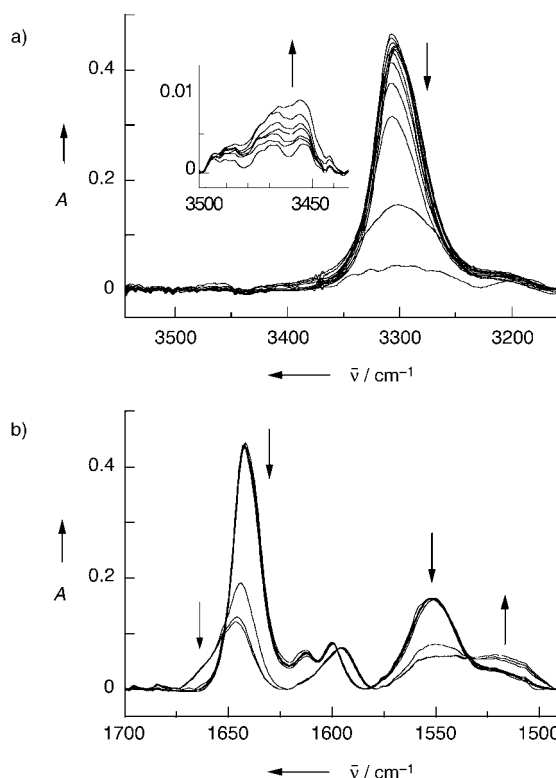


Figure 1. IR spectra of **1** gels in cyclohexane (2 wt %) at temperatures from 26 to 64 °C: a) ν_{NH} region, b) ester and amide I and II region.

confirm that hydrogen bonds between the amide groups contribute to the association process. We previously showed^[20] that compounds lacking the amide groups cannot aggregate in alkane solvents. Raising the temperature of the gel also strongly affects the molecular spectra (Figure 2). For example, the absorption band at 223 nm shifts to 207 nm and the bands at 264 and 258 nm transform into a single band at 251 nm. The UV spectrum of **1** in cyclohexane at higher temperatures is similar to the spectrum in chloroform (absorption bands at 254 and 308 nm, not shown). These modifications arise from π interactions between the aromatic rings. Such interactions also contribute to the self-assembly process. The presence of marked isosbestic points in the

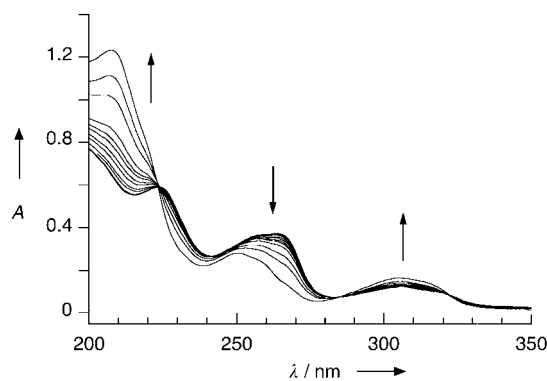


Figure 2. UV spectra of **1** gels in cyclohexane (0.3 wt %) at temperatures from 27 to 62 °C.

spectra shows that there is an equilibrium between aggregated and isolated species and that the position of this equilibrium depends on the temperature. Also, the intermediate species which lie between infinite aggregates and single molecules must have the same molar extinction coefficient. This would not be the case for the smallest aggregates, which would be expected to exhibit spectra which are different from both single molecules and larger aggregates. The stable isosbestic points, therefore, strongly suggest that the major intermediates comprise an equilibrium mixture of large aggregates.

The structure of the gels in cyclohexane has been investigated by electron microscopy (Figure 3). The gel was rapidly frozen to keep the solvent matrix in an amorphous state. Samples were fractured and Pt-shadowed (Figure 3a). Direct TEM could not be used because of the sample thickness and presence of organic solvent. This study revealed that the gels comprise cylindrical aggregates with a very large aspect ratio: their lengths are of the order of a micrometer, and their widths are about 20–30 nm with little dispersity. In a few samples the fracture occurred in a plane perpendicular to the cylinders axis, thus showing their cross-sections (Figure 3b). The white spot in the middle of the cylinder corresponds to an area that cannot be reached by the metal particles, and shows that it is lower than the surrounding rim. The cylinders are therefore hollow. The wall thickness was estimated from longitudinal fractures to be (4 ± 3) nm, the high uncertainty resulting mainly from the thickness of the evaporated metal. No branching structures were observed. Diluted solutions of **1** (below the concentration resulting in the gel) were rotary shadowed after deposition on carbon grids (Figure 3c) and found to contain mainly helical tapes. The mean diameter of those helices is (30 ± 4) nm, which lies in the same range as that of the cylinders. Tubules with helical defects can also be observed in the same solutions. They represent the last step of the self-assembly process, before the formation of the perfectly closed tubes, and emphasize again the link between the closed tubes and helical tapes. As the concentration increases, the lateral width of the helical tapes increases until the tubes are closed. In these samples, right-handed and left-handed helices are present in equal quantities, thus resulting in an overall racemic mixture. A few features structurally different to those discussed above were identified as ribbons. Their thickness was equal to that of the cylinders and they represent the first stage of tube formation.

Small-angle scattering experiments provided definitive evidence of the existence of the proposed tubular structure. The technique has been used successfully to elucidate the structure of nanotubes.^[14,21] We recorded the intensities of neutron scattering by low concentration **1**/[D₁₂]cyclohexane gels in the range of $q = 0.008\text{--}0.6 \text{ \AA}^{-1}$ (Figure 4). When interparticle correlations are negligible, the intensity scattered by a sample is given by Equation (1), in which Φ_v is the

$$I(q) = \Phi_v \Delta\rho^2 V_p P(q) \quad (1)$$

volume fraction of the particles, V_p is the volume of one particle (\AA^3), $\Delta\rho^2$ is the contrast of the particle (cm^{-4}), and $P(q)$ is the form factor of the particle. Figure 4 represents the

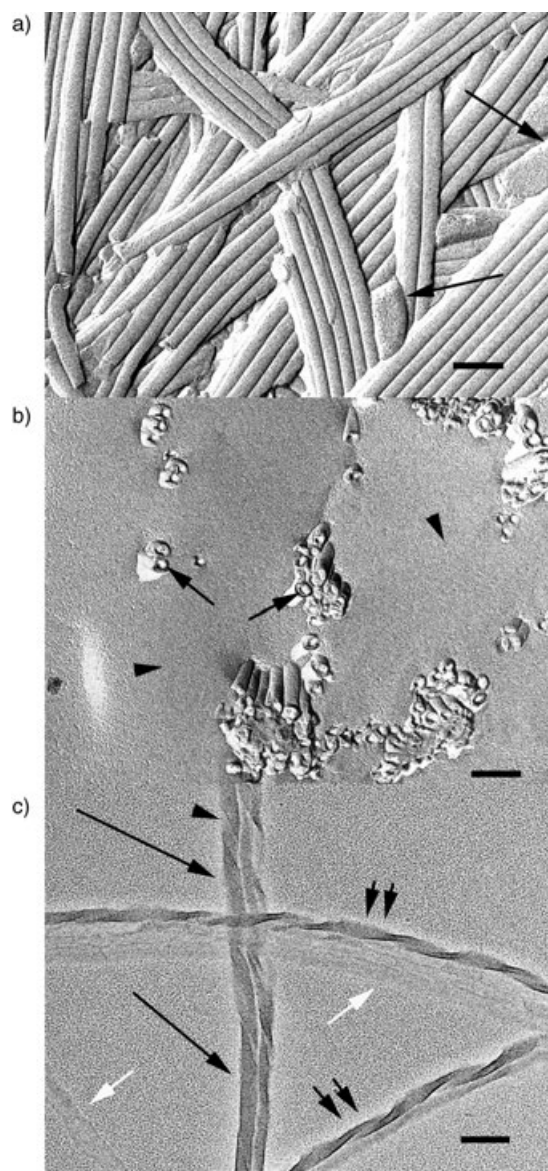


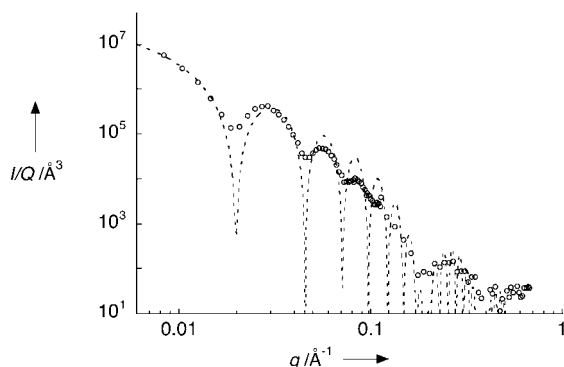
Figure 3. Electron micrographs of self-assembled **1** in cyclohexane. Scale bar is 100 nm. a) Replica of a freeze fracture of **1**-cyclohexane gels (2 wt% concentration). Diameters of the tubes approximately 25–30 nm. Arrow: solvent area. b) Same as (a) with a fracture plane nearly perpendicular to the main axis of the tubes. Arrows: sections of the tubes, which are clearly hollow. Arrowheads: amorphous solvent. c) TEM image of adsorbed diluted solution of **1** in cyclohexane (0.01 wt%) and rotary shadowed. White arrow: single tape. Double arrow: helical tape with a helical pitch of 120 nm. Long arrow: tubule showing only helical groove (arrow head).

intensity normalized to the contrast and the volume fraction as a function of the scattering vector q .

The form factor for a long cylinder^[22] can be approximated by Equation (2), where L is the length, R_o and R_i are

$$P(q) = \frac{\pi}{qL} \frac{4(R_o J_1(q R_o) - R_i J_1(q R_i))^2}{q^2 (R_o^2 - R_i^2)^2} \quad (2)$$

the outer and inner radii of the cylinder, respectively, and J_1 is the Bessel function of the first order. The first factor



- [11] D. S. Chung, G. B. Benedek, F. M. Konikoff, J. M. Donovan, *Proc. Natl. Acad. Sci. USA* **1993**, *90*, 11341.
- [12] a) D. A. Frankel, D. F. O'Brien, *J. Am. Chem. Soc.* **1994**, *116*, 10057; b) G. John, M. Masuda, Y. Okada, K. Yase, T. Shimizu, *Adv. Mater.* **2001**, *13*, 715.
- [13] J. H. Fuhrhop, D. Spiroski, C. Boettcher, *J. Am. Chem. Soc.* **1993**, *115*, 1600.
- [14] P. Terech, Y. Talmon, *Langmuir* **2002**, *18*, 7240.
- [15] a) S. Vauthey, S. Santoso, H. Gong, N. Watson, S. Zhang, *Proc. Natl. Acad. Sci. USA* **2002**, *99*, 5355; b) C. Valery, M. Paternostre, B. Robert, T. Gulik-Krzywicki, T. Narayanan, J. C. Dedieu, G. Keller, M. L. Torres, R. Cherif-Cheikh, P. Calvo, F. Artzner, *Proc. Natl. Acad. Sci. USA* **2003**, *100*, 10258.
- [16] J. P. Hill, W. Jin, A. Kosaka, T. Fukushima, H. Ichihara, T. Shimomura, K. Ito, T. Hashizume, N. Ishii, T. Aida, *Science* **2004**, *304*, 1481.
- [17] N. Nakashima, S. Asakuma, T. Kunitake, *J. Am. Chem. Soc.* **1985**, *107*, 509.
- [18] a) J. V. Selinger, F. C. MacKintosh, J. M. Schnur, *Phys. Rev. E* **1996**, *53*, 3804; b) C. M. Chen, *Phys. Rev. E* **1999**, *59*, 6192; c) A. Aggeli, I. A. Nyrkova, M. Bell, R. Harding, L. Carrick, T. C. B. McLeish, A. N. Semenov, N. Boden, *Proc. Natl. Acad. Sci. USA* **2001**, *98*, 11857; d) I. A. Nyrkova, A. N. Semenov, A. Aggeli, M. Bell, N. Boden, T. C. B. McLeish, *Eur. Phys. J. B* **2000**, *17*, 499.
- [19] a) K. Tomioka, T. Sumiyoshi, S. Narui, Y. Nagaoka, A. Iida, Y. Miwa, T. Taga, M. Nakano, T. Handa, *J. Am. Chem. Soc.* **2001**, *123*, 11817; b) J. Schneider, C. Messerschmidt, A. Schulz, M. Gnade, B. Schade, P. Luger, P. Bombicz, V. Hubert, J. H. Fuhrhop, *Langmuir* **2000**, *16*, 8575.
- [20] R. Schmidt, F. B. Adam, M. Michel, M. Schmutz, G. Decher, P. J. Mesini, *Tetrahedron Lett.* **2003**, *44*, 3171.
- [21] a) K. Sakurai, Y. Ono, J. H. Jung, S. Okamoto, S. Sakurai, S. Shinkai, *J. Chem. Soc. Perkin Trans. 2* **2001**, 108; b) T. Imae, K. Funayama, M. P. Krafft, F. Giulieri, T. Tada, T. Matsumoto, *J. Colloid Interface Sci.* **1999**, *212*, 330.
- [22] J. M. Deutch, *Macromolecules* **1981**, *14*, 1826.
- [23] S. Svenson, J. Koenig, J. H. Fuhrhop, *J. Phys. Chem.* **1994**, *98*, 1022.
- [24] R. Schmidt, M. Schmutz, A. Mathis, G. Decher, M. Rawiso, P. Mésini, *Langmuir* **2002**, *18*, 7167.
- [25] R. Schmidt, M. Schmutz, M. Michel, G. Decher, P. Mésini, *Langmuir* **2002**, *18*, 5668.
